Annals of Biomedical Engineering, Vol. 50, No. 4, April 2022 (© 2022) pp. 440–451
https://doi.org/10.1007/s10439-022-02928-x

Original Article

Smooth Muscle Organization and Nerves in the Rat Vagina: A First Look Using Tissue Clearing and Immunolabeling

Alyssa J. Huntington,[1] Barath Udayasuryan,[2] Pang Du,[3] Scott S. Verbridge,[2] Steven D. Abramowitch,[4] and Raffaella De Vita[1]

[1]STRETCH Lab, Department of Biomedical Engineering and Mechanics, Virginia Tech, 330A Kelly Hall, 325 Stanger Street, Blacksburg 24061, VA, USA; [2]Department of Biomedical Engineering and Mechanics, Virginia Tech, 330 Kelly Hall, 325 Stanger Street, Blacksburg 24061, VA, USA; [3]Department of Statistics, Virginia Tech, 417A Hutcheson Hall, 250 Drillfield Drive, Blacksburg 24061, VA, USA; and [4]Translational Biomechanics Lab, Department of Bioengineering, University of Pittsburgh, Benedum Hall, 3700 O'Hara Street, Pittsburgh 15213, PA, USA

(*Received 29 September 2021; accepted 6 February 2022; published online 19 February 2022*)

Associate Editor Joel D. Stitzel oversaw the review of this article.

Abstract—Smooth muscle fibers within the vagina, as well as the nerve fibers that contribute to their control mechanisms, are important for the maintenance and alteration of vaginal length and tone. Vaginal smooth muscle (VaSM) is typically described as being arranged into two distinct concentric layers: an inner circular muscular layer and an outer longitudinal muscular layer. However, the distribution of VaSM oriented in the longitudinal direction (LD) and circumferential direction (CD) has never been quantified. In this study, tissue clearing and immunohistochemistry were performed so that the VaSM, and surrounding nerves, within whole rat vaginas ($n = 6$) could be imaged without tissue sectioning, preserving the three-dimensional architecture of the organs. Using these methods, the vagina was viewed through the full thickness of the muscularis layer, from the distal to the proximal regions. The VaSM orientation in the proximal and distal regions and the VaSM content along the LD and CD were quantified. Additionally, a qualitative assessment of vaginal nerves was performed. When compared using a permuted version of the Watson U^2 test, the orientation of VaSM in the proximal and distal regions were found to be significantly different in 4 of the 6 imaged rat vaginas ($p = 0.000$). While the distal vagina contained a similar amount of VaSM oriented within $\mp 15^\circ$ of the LD and within $\mp 15^\circ$ of the CD, the proximal vagina contained significantly more VaSM oriented towards the LD than towards the CD. Nerve fibers were found to be wavy, running both parallel and perpendicular to vascular and non-vascular smooth muscle within the vagina. Micro-structural analyses, like the one conducted here, are necessary to understand the physiological function and pathological changes of the vagina.

Keywords—Vagina, Smooth muscle, Innervation, Tissue clearing, Immunohistochemistry, Confocal microscopy.

INTRODUCTION

The vagina is an essential organ of the female reproductive system, connecting the uterus to the outside of the body for menstruation, conception, and birthing. Within the female pelvis, the vagina is positioned between the bladder and the rectum and supported by a complex network of pelvic muscles and ligaments. This reproductive organ experiences intense forces and large deformations during major events like pregnancy and vaginal delivery, in addition to undergoing significant mechanical changes in everyday life. These changes are determined by intra-abdominal pressure and posture,[8] the filling of the bladder and rectum,[10] sexual arousal,[19] and intercourse.[14] The exact mechanisms of the mechanical feats of the vagina remain unclear, though vaginal smooth muscle (VaSM) and innervation play, without any doubt, a significant role. Controlled by nerves, smooth muscle relaxes and contracts to accommodate alterations in the length and caliber of the vagina, thus contributing to the organ's ability to modulate stresses and strains. However, much remains unknown about the micro-structural organization of VaSM and its innervation.

Address correspondence to Raffaella De Vita, STRETCH Lab, Department of Biomedical Engineering and Mechanics, Virginia Tech, 330A Kelly Hall, 325 Stanger Street, Blacksburg 24061, VA, USA. Electronic mail: devita@vt.edu

The vagina has a thick muscularis layer, which is typically described as containing smooth muscle cells oriented along the circumferential direction (CD) and longitudinal direction (LD) (Fig. 1a). The morphology of the muscularis is thought to vary along the length of the vagina, though there is not consensus in this regard. For example, studies investigating VaSM distribution using rats of similar size and age have reported that the vagina contains higher percentage and more densely packed smooth muscle in the proximal region than in the distal region,[3,45] as well as a thicker smooth muscle layer in the distal region than the proximal region.[17,39] The presence of smooth muscle oriented along the LD and CD allows the vagina to generate contractions along each of these anatomical directions. However, the full extent of the functional purposes of longitudinal and circumferential VaSM activity is not well understood.

The differences in *ex-vivo* contractile forces generated along the LD and CD have been quantified experimentally by several investigators.[11,17,24,25,38] Planar biaxial and inflation–extension contractile tests revealed that high potassium-induced contractions are stronger along the LD than along the CD.[11,24,26] This indicates that there may be more smooth muscle oriented in the LD compared to the CD. However, besides reports of a circumferentially oriented sphincter-like structure in the rat distal vagina,[17,45] histological studies about VaSM content typically describe the muscularis as a whole, most commonly by reporting the fractional area of muscle within the muscularis,[4,5,49,50,52] rather than distinguishing between LD and CD oriented muscle or quantifying local smooth muscle alignment.

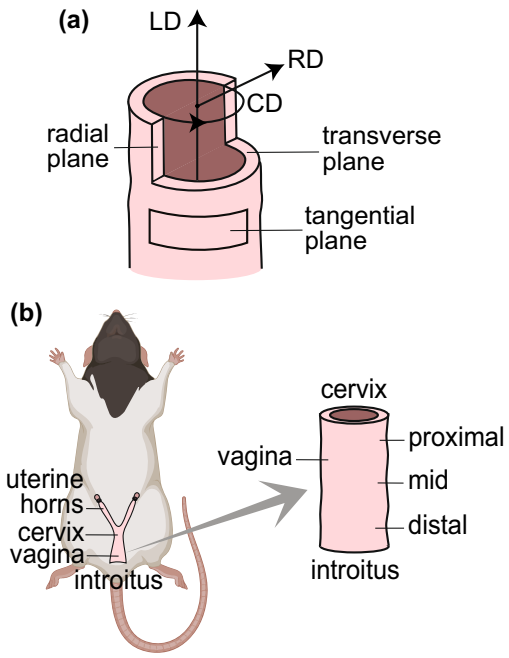

FIGURE 1. (a) Radial, tangential, and transverse planes and radial direction (RD), longitudinal direction (LD), circumferential direction (CD) of the vagina. (b) Rat vagina with proximal (closer to the cervix), mid, and distal (closer to the introitus) regions.

The neural pathways that control smooth muscle tone in the vagina, both in the muscularis and in the vasculature, are still not well understood, but there is evidence that cholinergic, adrenergic, and nonadrenergic–noncholinegic nerves all contribute to such control mechanisms.[17,18] A higher density of nerves has been found in the anterior vagina compared to the posterior vagina, as well as in the distal vagina compared to the proximal vagina in human biopsies and cadaveric tissue.[22,46] However, innervation has also been found to not vary significantly along the length of the rat vagina[45] and along the length of the human anterior vagina.[34] The nerve distribution with respect to VaSM is likely to play a role in vaginal contractility.

Smooth muscle content within the vaginal wall varies throughout a woman's life. During pregnancy, VaSM cells undergo changes in phenotype, likely as mechanism to alter the material properties of vaginal tissue in preparation for delivery.[13] After menopause, VaSM content decreases and vaginal atrophy increases.[42] Similarly, VaSM content decreases in women suffering from pelvic organ prolapse, a pelvic floor disorder characterized by the descent of organs into the vaginal canal.[4,5,27,50,53] Nerve density is also lower in the vaginal wall of women with pelvic floor disorders.[5,27,29,55] In addition, surgical meshes for the treatment of pelvic organ prolapse have a negative impact on VaSM functionality.[15,16,28,30,44] It is still unclear, however, whether smooth muscle alterations associated with pregnancy, aging, pelvic organ prolapse, and mesh implantation are more pronounced in one anatomical direction than another or whether the smooth muscle is affected equally, independently of the anatomical location.

To date, all histological descriptions of VaSM and all but one[40] description of vaginal nerve distribution have been derived from histological analysis of thin (4 μm[5,11,27,50] to 15[46] μm) sections of the vagina. Thin sections are typically used to allow the penetration of light during microscopy. While the images of these sections can provide important information regarding the overall content of the tissue, they cannot easily capture the three-dimensional architecture of the tissue. For example, sections in the transverse plane (Fig. 1a) only show smooth muscle and nerve fibers that are aligned along the CD and the cross-sections of such fibers that are oriented along LD. Similarly sections in the radial plane can capture the smooth muscle and nerve fibers aligned along the LD but only the cross-section of these components that are oriented

along the CD (Fig. 1a). In order to measure the orientations of smooth muscle and nerve fibers, ideally one should view the tangential plane of the tissue such that both the LD and CD are in-plane (Fig. 1a). However, sections in the tangential plane are difficult to obtain, especially from the vaginas of small animals, because the vaginal wall is thin (0.38±0.13 mm[26]). Regardless of where the tissue sections are cut, if smooth muscle bundles or nerves are not perfectly aligned in the plane of the sections, the collected images will reveal primarily oblique cross-sections of these components. Furthermore, thin sections present only a narrow view of the tissue, and disturb the three-dimensional architecture of the smooth muscles and nerves. To gather more precise orientation data of smooth muscle and better describe nerves, the vaginal tissue should remain intact and not be sectioned.

In this study, we quantified the orientation of smooth muscle within the vaginal wall, and identified variations of smooth muscle content with respect to anatomical region. Additionally, we performed a qualitative assessment of nerves throughout the vagina. We hypothesized that a higher proportion of smooth muscle would be oriented along the LD than along the CD since stronger contractions in response to KCl have been observed along the LD.[24] By performing tissue clearing, which increased the transparency of the tissue such that the vaginal walls could be imaged through their thickness without sectioning, and antibody labeling, we were able to image the smooth muscle and nerves. The results presented here offer insight towards the contractile properties of the vagina, which are impacted by pregnancy, aging, pelvic floor disorders, and surgical mesh intervention for prolapse.

METHODS

Tissue Clearing and Immunohistochemistry

Female Long Evans virgin rats aged 75–105 days ($n = 6$) were sacrificed *via* decapitation following the Institutional Animal Care and Use Committee (IACUC) guidelines at Virginia Tech. Full length vaginas were immediately dissected from the rats and were kept intact, except to remove the cervix and skin surrounding the introitus (Fig. 1b). The urethra was carefully separated from the vagina using dissection scissors. A suture was passed through the proximal ventral vagina and knotted so that the anatomical regions could be identified throughout the clearing and imaging process. Once excised, the vaginas were approximately 10–15 mm in length and 5–10 mm in diameter.

The rat vaginas were fixed in 10% formalin at 4 °C overnight before being subjected to a tissue clearing protocol using a tissue clearing kit (ab243298, Abcam, UK). Briefly, the fixed organs were first washed with phosphate buffered saline (PBS), and then dehydrated by immersing the organs in increasing concentrations of methanol: 50% methanol in PBS, 80% methanol in deionized (DI) water, and 100% methanol, each for 16 min at 4 °C. The organs were then rehydrated using a decreasing concentration of methanol: 20% dimethylsulfoxide (DMSO) and 80% methanol, 80% methanol in DI water, 50% methanol in PBS, and 100% PBS), each for 30 min at room temperature. Next, the vaginas were permeabilized in a solution of PBS with 0.2% Triton X for 30 min and incubated with a penetration buffer for 1 h and a blocking buffer for 3–4 h. The specimens were subsequently incubated with primary rabbit α-smooth muscle actin antibody, mouse CD31 monoclonal antibody, and chicken anti-PGP 9.5 polyclonal antibody in a solution of antibody buffer overnight. Specimens were then washed with washing buffer five times for 30 min each. Goat anti-Rabbit IgG, goat anti-Mouse IgG, and goat anti-Chicken IgG were used as the secondary antibodies for fluorescence. Specimens were incubated with the secondary antibodies and diamidino-2-phenylindole (DAPI) (1:1000 of 10 mg/mL) for 3 h at 37 °C. Note that all $n = 6$ rat vaginas were stained for α-smooth muscle actin, vascular endothelial cells (and cell nuclei), and 3 of those 6 were also stained for nerves. Details regarding the specific antibodies and concentrations used in this study are shown in Table 1.

The stained specimens were washed with washing buffer ten times, each for 15–90 min at 37 °C. They were then dehydrated using solutions of 50% methanol in PBS, 80% methanol in DI water, and 100% methanol, each for 16 min at 4 °C. Finally, the specimens were cleared by incubating them in Tissue Clearing Reagent 1 (Abcam, UK) for 2 h followed by Tissue Clearing Reagent 2 (Abcam, UK) for 2 h. Cleared

TABLE 1. Immunohistochemistry antibodies used to stain rat vaginas (Color figure online).

	α-Smooth Muscle Actin	Vascular Endothelial Cells	Nerves
Primary Antibody	Rabbit anti-αSMA	Mouse anti-CD31	Chicken anti-PGP 9.5
Product Details	ab5694 Abcam	MA1-80069 Invitrogen	PA1-10011 Invitrogen
Concentration	1:200	1:200	1:500
Specimen Number	6	6	3

Secondary Antibody (Fluorophore)	Goat anti-Rabbit (488)	Goat anti-Rabbit (647)	Goat anti-Mouse (647)	Goat anti-Mouse (488)	Goat anti-Chicken (568)
Product Details	ab150077 Abcam	A24245 Invitrogen	A32728 Invitrogen	A11001 Invitrogen	A11041 Invitrogen
Concentration	1:100	1:1000	1:100	1:1000	1:5000-1:1000
Specimen Number	3	3	3	3	3

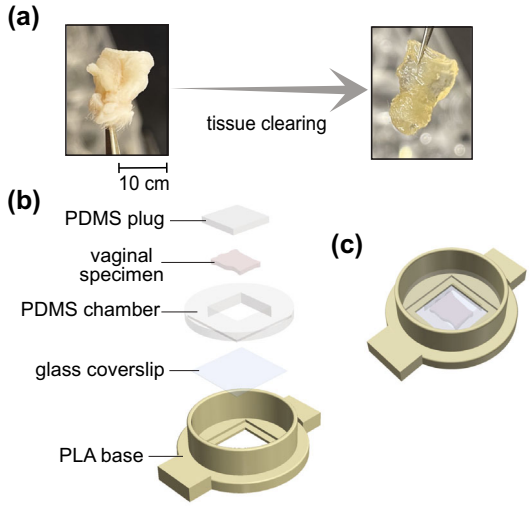

FIGURE 2. (a) Rat vagina specimen before and after tissue clearing. (b) Components of the custom-made chamber used to hold vaginal specimens for imaging. (c) Assembled custom-made chamber.

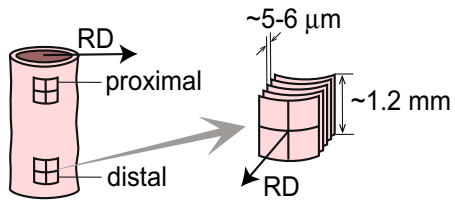

FIGURE 3. Schematics of the proximal and distal stacks of 4-tiled images in each rat vagina. Each stack containing images collected at several (from 30 to 50) radial locations. These images were analyzed to measure the VaSM orientation in the proximal and distal vagina.

tissue was stored at 4 °C in Tissue Clearing Reagent 2 in the dark (Fig. 2a).

Image Acquisition

After clearing and staining, rat vaginas were mounted in a custom-made chamber comprised of a 3D printed polylactic acid (PLA) base, a glass coverslip, a polydimethylsiloxane (PDMS) chamber with a PDMS plug (Fig. 2b). Whole vaginal specimens were placed in the chamber such that either the ventral or dorsal side of the vagina was flat against the glass coverslip, and was held in this position by the PDMS chamber and plug (Fig. 2c). Fluorescence microscopy was performed on a Zeiss LSM 800 confocal microscope at ×10 magnification and ×20 magnification. The entire volume of the specimen was panned across so that preliminary qualitative observations regarding the smooth muscle and nerve distributions could be made.

High-resolution images were captured using the tiling functionality of the confocal microscope to visualize smooth muscle and nerve architecture. However, measurements of VaSM orientation were only performed on images that contained large visible amounts of smooth muscle. The analyzed images were comprised of 4 (2×2) tiles stitched together to form a region with approximate dimensions of 1200 μm ×1200 μm (Fig. 3). No images were analyzed from the mid region to measure VaSM orientation since VaSM content was not significant. For each of the vaginal specimens ($n = 6$), both the proximal region and the distal region were selected for VaSM orientation measurements (Fig. 3a), for a total of 12 analyzed regions. Within each region, z-stack images were acquired at increments of 5–6 μm such that the vagina could be imaged through the entire thickness. This resulted in a minimum of 37 and a maximum of 52 images collected along the RD in each of the 12 imaged regions, for a total of 503 images that were analyzed for VaSM orientation measurements.

To confirm that the muscularis could be imaged through the entire thickness, after z-stacks images from the abluminal side of one specimen were captured as described above, the specimen was inverted, re-mounted in the custom-made chamber with the luminal side against the glass coverslip, and z-stacks images were collected. The images of the same regions from both the abluminal and luminal sides of the vagina were compared, confirming the presence of smooth muscle with the same features.

Images were acquired to visualize the innervation of the rat vagina. Smaller images (tiles) and larger (tiled images) of innervation were taken at random locations, including regions in which nerves surrounded vasculature and regions in which nerves surrounded non-vascular smooth muscle, at ×10 and ×20 magnification.

Image Analysis

The tiled z-stack images containing dense smooth muscle content were exported as a series of individual images such that each image represented the vaginal tissue at a single radial depth. The alignment of α-smooth muscle actin in each image was computed using an open source software, CurveAlign v4.0[7,6] in MATLAB (Fig. 4). This software quantifies all fiber angles within a region of interest relative to a user defined boundary. It removes noise from images using fast discrete curvelet transforms[9] and extracts individual fibers using the fiber extraction (FIRE) algorithm.[48] It should be noted that vasculature, which also

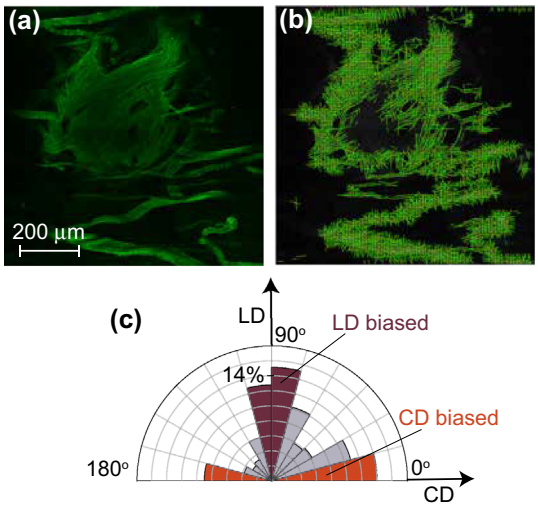

FIGURE 4. (a) Two-dimensional view of smooth muscle in the proximal region of one vaginal specimen at one radial depth. (b) Overlay image showing the orientation of smooth muscle and (c) corresponding polar histogram of the output orientation data obtained using the CurveAlign software. Magnification: ×10

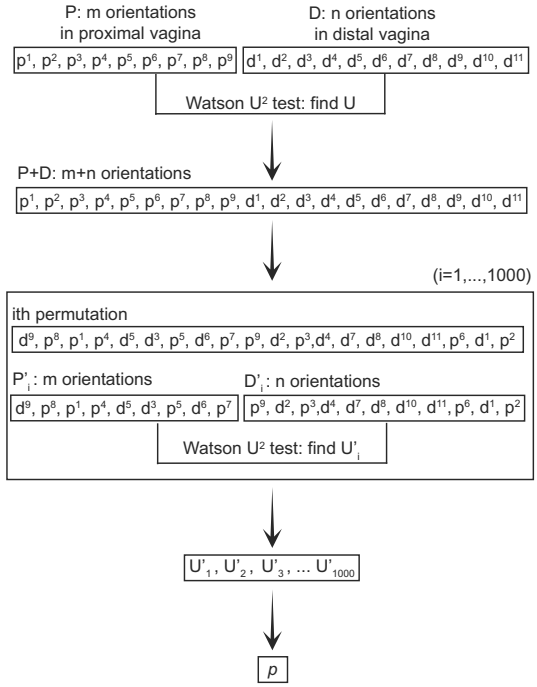

FIGURE 5. Schematics of statistical methods used to compare differences between VaSM orientation between the distal and proximal vaginas. For the example shown, $m = 9$ and $n = 11$.

contains α-smooth muscle actin, was not excluded from analysis, so alignment data included the orientation of smooth muscle within the muscularis as well as vascular smooth muscle. Orientation data of one (proximal or distal) region calculated at several radial depths were combined to describe the orientation of smooth muscle of the region.

Smooth muscle with an orientation value between −15° and +15° of the LD was defined as "LD biased" and smooth muscle with an orientation value between −15° and +15° from the CD was defined as "CD biased," following the definition presented by Nagatomi *et al.*[37] (Fig. 4c). The percentages of LD and CD biased smooth muscle within the proximal and distal regions of each vaginal specimen were calculated. Additionally, such percentages were combined to generate percentages of LD and CD biased smooth muscle across the entire vaginal specimen.

Statistical Analysis

For each vaginal specimen, the orientation values of VaSM in the proximal and distal regions were statistically compared by means of a permuted version of a Watson U^2 test[32,54] using the circular package[1] of the R statistical software[41] (Fig. 5). The permuted version of the Watson U^2 test, rather than the standard one, was used to overcome the requirement of independent sets of data, as the two sets of orientation values from the proximal and distal regions were derived from the same rat vaginal specimen and are likely correlated with each other. Briefly, the standard Watson U^2 test between the data set P from the proximal region, with m number of orientation measurements, and the data set D from the distal region, with n number of orientation measurements, was performed to generate a test statistic value, U. Then, the data sets P and D were merged for each specimen and the orientation measurements of this merged set were randomly permuted. After the ith random permutation, the first m orientation values of the permuted set was used to form a new data set P'_i while the last n orientation values formed a new data set D'_i. A Waston U^2 test was performed between P'_i and D'_i to generate a test statistic value, U'_i. This procedure was repeated 1000 times for a total of 1000 permutations, resulting in a group of 1000 permutation test statistic values $U'_1, .., U'_{1000}$. The original test statistic value U, which described the difference between the proximal and distal VaSM orientations, was compared with these 1000 test statistic values (Fig. 5). The probability of obtaining a permutation test statistic value larger than U was computed as:

$$p = \frac{1}{1000}\sum_{i=1}^{1000}\gamma_i \quad \text{with} \quad \gamma_i = \begin{cases} 1 & U'_i \geq U, \\ 0 & U'_i < U. \end{cases} \qquad (1)$$

This probability was taken to be the p-value for the statistical test. If two data sets were different from each other, the chance that randomly permuted data would

result in a larger test statistic value than U would be small. Note that we performed six comparisons here, so a multiple comparison adjustment was necessary. More precisely, we used the significance level of $\alpha = 0.05$ and the Bonferroni correction procedure where the p-value was compared with $0.05/6 = 0.008$, with a p-value lower than this value indicating that the orientations of these two groups were significantly different in the statistical sense.

In addition to comparing the overall VaSM orientation between the proximal and distal regions, LD and CD biased smooth muscle data within the proximal vagina, the distal vagina, and the entire (proximal plus distal) vaginas were compared. These data were normally distributed, as determined by Shapiro-Wilk test for normality, except for the percentage of LD biased smooth muscle in the distal region ($p = 0.019$). Wilcoxon Sign-Rank tests were performed to compare the percentage of LD biased smooth muscle to the percentage of CD biased smooth muscle in the distal region, proximal region, and overall vagina. For this comparison, the statistical significance was set to 0.05.

RESULTS

The tissue clearing process was successful in increasing the transparency of the vaginal specimens so that images could be collected throughout the entire radial depth of the muscularis (Fig. 6a). Vascular smooth muscle was easily distinguished from non-vascular smooth muscle by its structure as well as its proximity to vascular endothelial cells. Vascular smooth muscle tended to be closer to the abluminal side than non-vascular smooth muscle, though it was also interwoven throughout the muscularis. Vascular smooth muscle was observed as close as 5–20 μm from the abluminal side of the tissue (Fig. 6b), whereas non-vascular smooth muscle typically was found at a distance of 50–100 μm from the abluminal side (Fig. 6c).

The proximal, mid, and distal regions of the vaginal specimens all contained smooth muscle with unique structural features within the muscularis. In the proximal vagina, a dense network of easily distinguishable, thick, and interweaving smooth muscle bundles was observed in all six specimens. In the mid region, smooth muscle bundles tended to be thinner and more dispersed. Non-vascular muscle in the mid region tended to present as thin, short, and circumferentially oriented segments. The distal region contained more smooth muscle than the mid region, but bundles were not as plentiful or as easily distinguishable as those in the proximal region. A circumferentially oriented band of muscle, similar to the sphincter like structure described by others,[17,45] was observed in the distal region of all six specimens. Examples of these regional variations for three representative vaginal specimens are displayed in Fig. 7. Smooth muscle content also varied between the ventral and dorsal sides of the vagina, with all of the specimens appearing to contain significantly more muscle in the dorsal vagina.

The orientation distributions of VaSM in the proximal and distal regions of the dorsal side of all vaginal specimens are presented in Fig. 8. These distributions were bi-modal, with peaks along both the

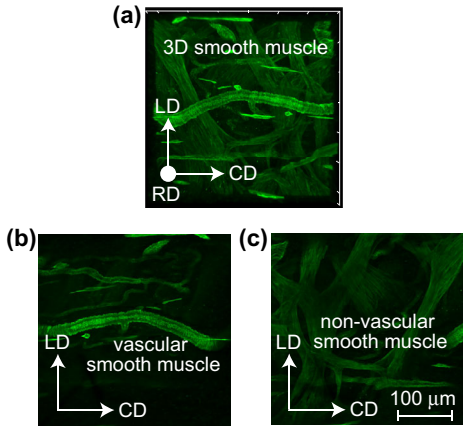

FIGURE 6. (a) Three-dimensional view of smooth muscle of one vaginal specimen. (b) Two-dimensional view of vascular smooth muscle at one radial location, closer to the abluminal side and (c) non-vascular smooth muscle at another radial location, closer to the luminal side of the same specimen. Magnification: ×10.

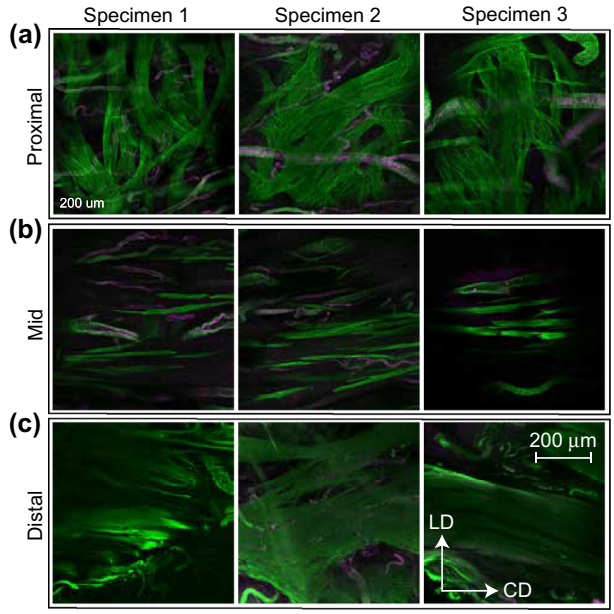

FIGURE 7. Two-dimensional view of (a) proximal regions, (b) mid regions, and (c) distal regions of three representative vaginal specimens at single radial depths. Green represents α-smooth muscle actin and purple represents vascular endothelial cells. Magnification: ×10.

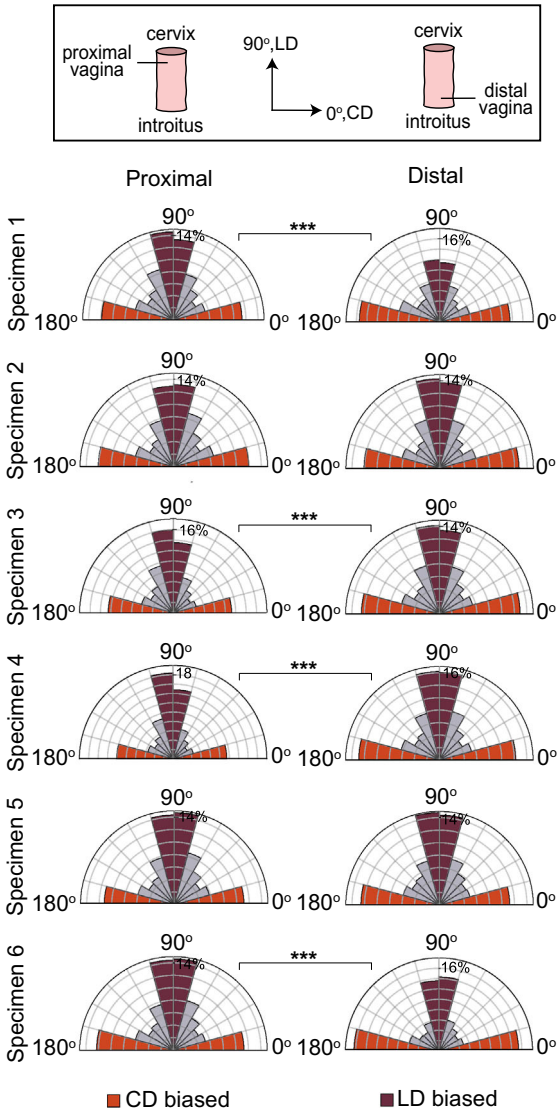

FIGURE 8. Statistical comparison of polar histograms of VaSM orientations in the proximal and distal regions of all $n = 6$ vaginal specimens throughout their entire depth. ***$p = 0.000$.

CD (0°) and LD (90°). Images for each region were processed as an entire stack of images, capturing the entire depth of the muscularis. In each anatomical region, the distribution of smooth muscle angles contained a higher proportion of values within ∓15° of the CD (0° and 180°) and LD (90°) than in any other direction. Permuted Watson U^2 tests revealed significant differences between the orientation distributions of smooth muscle in the distal and proximal regions in 4 out of the 6 specimens ($p = 0.000$), but similar distributions in 2 of the specimens ($p = 0.661$ and $p = 0.620$) (Fig. 8).

The proportions of smooth muscle oriented within ∓15° of either the CD or the LD are displayed in

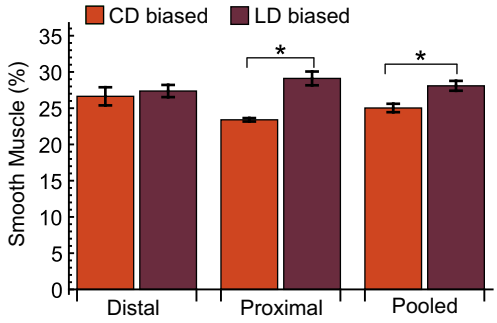

FIGURE 9. Mean smooth muscle content (%) oriented within ∓15° of the LD and CD within the distal and proximal regions, as well as the entire vagina. Error bars represent standard error. *$p < 0.05$.

Fig. 9. In the distal region, there was no significant difference between the proportions of CD and LD biased smooth muscle ($p = 0.917$). The distal region contained 26.64 ± 1.25% of smooth muscle biased towards the CD and 27.37 ± 0.84% of smooth muscle biased towards the LD. In the proximal region, there was significantly more LD biased smooth muscle than CD biased smooth muscle ($p = 0.027$); 23.40 ± 0.24% of smooth muscle was biased towards the CD and 29.11 ± 0.95% of smooth muscle was biased towards the LD. When data from both regions were combined together to generate pooled data sets, there was significantly more smooth muscle that was LD biased than CD biased ($p = 0.046$). The pooled data sets contained 25.03 ± 0.58% of smooth muscle biased towards the CD, and 28.09 ± 0.68% of smooth muscle biased towards the LD (Fig. 9) The percentage of LD biased smooth muscle was similar across all vaginal specimens ($n = 6$), varying by only 7.1% in the proximal region and by 5.9% in the distal region. Similarly, all specimens contained similar percentages of CD biased smooth muscle, which varied by 7.9% in the distal region and by 1.17% in the proximal region across the 6 specimens.

Nerves were found surrounding vasculature, interwoven throughout non vasculature smooth muscle, and in regions without smooth muscle. Nerve fibers were almost parallel and perpendicular to vascular and non-vascular smooth muscle (Fig. 10). Since the vaginal specimens were not sectioned, individual nerves could be followed over several millimeters throughout various radial depths of the tissue (Fig. 11a). Both thick bundles of nerves and thin single nerve fibers were observed (Fig. 11b). Nerve bundles and individual fibers both tended to be wavy, branching out from each other (Figs. 11c and 11d). While a quantitative analysis was not performed, it was consistently observed that the ventral vagina was more abundant in nerves that the dorsal vagina, the mid vagina contained

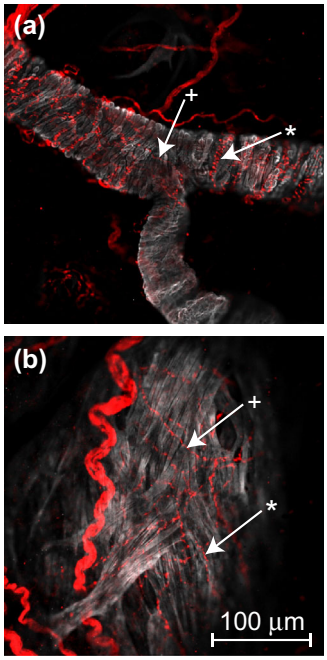

FIGURE 10. Two-dimensional view of nerves aligned along the smooth muscle fibers (∗) and perpendicular to the smooth muscle fibers (+) for (a) vasculature and (b) non vasculature smooth muscle. White represents α-smooth muscle actin and red represents nerves. Magnification: ×20.

fewer nerves than the proximal and distal regions. Moreover, nerves tended to be more abundant closer to the abluminal side than the luminal side.

DISCUSSION

In this study, we presented the first quantification of the smooth muscle architecture in the rat vagina by combining tissue clearing, antibody labelling, confocal microscopy imaging, and data analysis methods. The complex innervation of the organ was also visualized. By using tissue clearing techniques, we increased the optical transparency of vaginal specimens while preserving their three-dimensional organization. We obtained a complete view of the exact arrangement of the VaSM and nerves, without sectioning the vagina, *via* immunohistochemical staining. Images were acquired in the tangential plane of the vagina, containing both the main anatomical directions of the vagina, the LD and CD, at various radial depths. Orientations of the VaSM with respect to these directions, in both the proximal and distal regions, were determined, showing that the vagina has overall more smooth muscle in the LD than the CD. Nerve fibers and bundles appeared to be wavy and interwoven with vascular and non vascular smooth muscle.

Mechanical testing of the murine vagina has revealed that KCl-induced contractions are stronger in

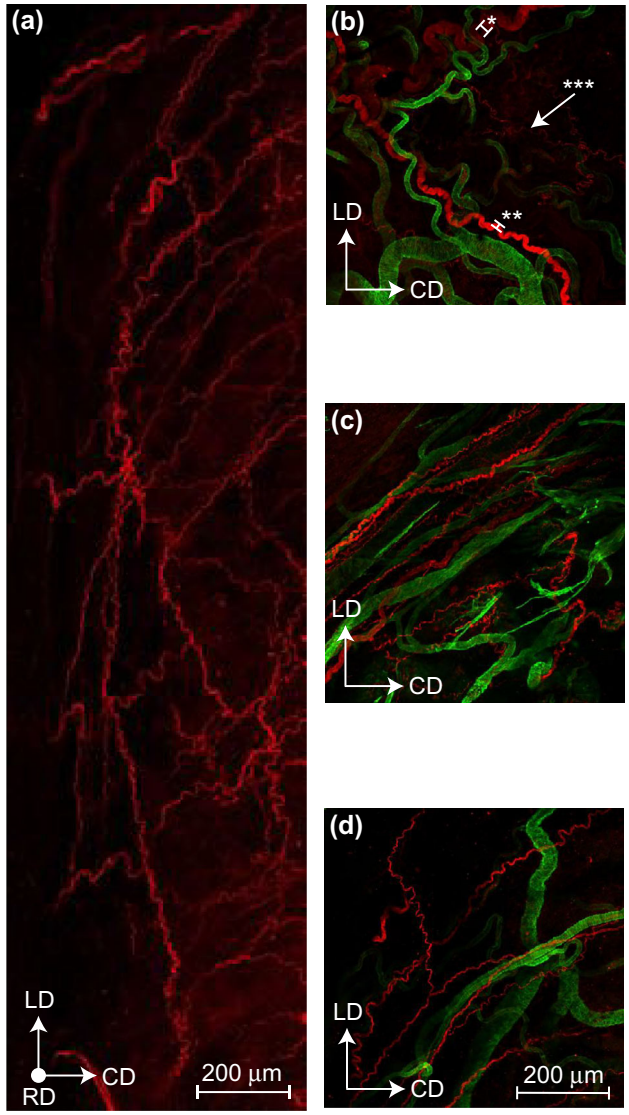

FIGURE 11. (a) Three-dimensional view of nerves spanning several millimeters, (b) two-dimensional view of thick bundles of nerves and thin individual nerve fibers at one radial depth (* = 25 μm, **10 μm, ***2 μm, and (c)–(d) two-dimensional view of wavy branches of vaginal nerves at single radial depths. Green represents α-smooth muscle actin and red represents nerves. Magnification: ×10.

the LD than the CD.[11,24–26] Recently, we have also reported that strains caused solely by contractions are larger in the proximal region compared to the distal region.[24] Together, these findings led us to hypothesize that there would be more smooth muscle oriented along the LD than the CD and more smooth muscle in the proximal region than in the distal region. This study confirmed that the organization of smooth muscle in the vagina varies with anatomical region (Figs. 7 and 8), with the proximal vagina having denser non-vascular smooth muscle that is organized into distinct bundles (Fig. 7). The VaSM orientation data

produced a bimodal distribution in both the proximal and distal vaginas, with the two peaks occurring along the angles corresponding to the LD and CD (Fig. 8). There was a significantly higher proportion of LD oriented smooth muscle than CD oriented smooth muscle in the proximal region and, overall, in the entire vagina (Fig. 9). The distal vagina contained a similar amount of smooth muscle oriented along both of these directions. Based on this investigation, we believe that the generation of higher contractions along the LD reported in our previous study[24] is due, at least in part, to larger quantities of smooth muscle fibers aligned in this direction. While the exact function of smooth muscle within the vagina remains unknown, VaSM is, without doubt, implicated in the maintenance of sexual function, preservation of vaginal tone, and compliance of the vagina. Therefore, our findings about significantly more VaSM oriented along the LD than CD may suggest that VaSM can modulate vaginal length more than vaginal diameter, especially in the proximal region.

While the muscularis is typically described as composed of two distinct layers, with VaSM primarily oriented along the LD in the outer layer and along the CD in the inner layer,[12] we did not observe any clear delineation between such layers. Rather, we noted interweaving smooth muscle bundles extending across the vaginal tissue. These results are consistent with the morphometric study of the human posterior vagina by Boreham *et al*[5] where the lack of a clear delineation between the outer longitudinal and inner circumferential smooth muscle layers was noted. Gruber *et al*[21] commented that the distinction between the muscularis layers in the swine vagina was most evident in mature animals. Since the rats used in this study were sexually mature but relatively young, future studies on vaginas from older rats should investigate whether the smooth muscle arrangement in layers changes with age.

We presented new images of vaginal nerves that had not been severed as typically done when preparing tissue slices for immunohistochemistry, offering an in-depth look at the intact morphology of nerves within the vaginal wall (Figs. 10 and 11). Several studies have been conducted to determine the neural pathways in vaginal tissue and their control mechanisms, revealing the presence of nitric oxide synthase, vasoactive intestinal polypeptide, neuropeptide Y, calcitonin gene-related peptide, and substance P in nerve fibers that extend throughout the length of the vagina.[23] Because we used a general neuronal marker (PGP 9.5 polyclonal antibody), we did not distinguish between the various types of nerves. We observed the largest amount of nerves in the ventral vagina, though such amount was not quantified in relation to the amount of nerves in the dorsal vagina. Nerve fibers were arranged almost parallel and perpendicular to smooth muscle, confirming previously reported data in the female mouse vagina.[20] The nerves appeared to be wavy with highly variable degrees of tortuosity. This waviness of vaginal nerves has been reported in other studies.[22,31] Hilliges *et al*[22] speculated that the nerve tortuosity serves to improve smooth muscle innervation but, as suggested by Krantz *et al*,[31] the waviness may likely serve to reduce neural loading during vaginal deformation. We attempted to quantify the orientation of nerve fibers. However, the waviness of nerve fibers made automated analysis of neural alignment challenging. The software used in this study presented only local alignment of nerve segments, failing to capture the overall orientation of the curvy nerves. Manual quantification was not feasible either, as it was challenging to trace individual nerves along their length in areas in which dozens of small and large fibers were close together and in areas where the nerves extended across the thickness of the vagina.

We reported, for the first time, orientation distributions of VaSM in both the proximal and distal regions of the rat vagina. These were found to be significantly different in 4 out of the 6 vaginal specimens that were analyzed (Fig. 8). Quantifying the VaSM orientation is an essential step towards the development of structurally-based constitutive models that aim to capture the anisotropic and inhomogeneous mechanical behavior that the vagina exhibits both in the passive state[35,36] and in the active state.[24,26] Existing constitutive models for the vaginal tissue include strain invariants to capture the anisotropy of the tissue in the passive state,[2,33] but they do not account for the VaSM contribution to the active mechanical response. Probability density functions that describe the VaSM orientation data collected here can be incorporated into structurally-based constitutive laws, as done by Tan and De Vita[51] to characterize the passive and active mechanical behavior of other soft tissues.

This study is not without limitations. First, while we did look at VaSM on both the dorsal and ventral sides of the vagina, we consistently found that the ventral side did not contain large regions of VaSM like the dorsal side did. Collected images of the ventral vagina typically presented large non-fluorescent dark regions with no smooth muscle. For this reason, we only performed quantitative analysis of VaSM in the dorsal vagina. Second, since the LD and CD of the vagina were the in-plane directions during imaging, the resolution of images in the tangential plane was much higher than the resolution of any image that could be digitally reconstructed along the RD by way of image stacks. Therefore, the orientation of VaSM in the radial and transverse planes could not be measured.

Third, both non-vascular and vascular smooth muscle were included in our quantification of VaSM orientation, and we could not isolate only the contribution of nonvascular smooth muscle. To visualize vasculature specifically, we stained the endothelial cells but the vasculature could not be "subtracted" from the images since α-smooth muscle actin and endothelial cells did not occupy the same pixel locations in the images. In addition, we did not focus on quantifying the vasculature within the rat vagina since this has been revealed in great detail using image analysis of vascular corrosion casts.[43] Finally, although we made every effort to preserve the micro-structure of the vagina, it is still possible that the configuration of smooth muscle and nerve fibers may have been slightly altered once the organ was isolated from the animal, when it was subjected to the tissue clearing protocol, or when it was confined in the custom-made chamber for imaging.

To date, all histological analysis of the vaginal muscularis has been performed from images of thin sections of the vaginal wall collected in the radial, transverse, or tangential plane. The methods that we propose here provided an in-depth larger view of the intact architecture of VaSM and nerves in healthy virgin rat vaginas. By adopting similar techniques, future studies should investigate how physiological processes and pathological conditions impact the whole rat vaginas. They should explore to which extent the three-dimensional organization of the vaginal micro-structure is altered following pregnancy, menopause, or the development of pelvic floor disorders.

Whether rats (and other quadrupeds) can be used to study the tissue micro-structure of the vagina and its alterations due to pregnancy, menopause, pelvic floor disorders in humans is a contentious issue. It is possible that the difference in smooth muscle content between the ventral (or anterior) and dorsal (or posterior) regions of the vagina that we observed in rats is not present in humans. The vagina may be richer of smooth muscle in the dorsal region only in rats (and, possibly, other quadrupeds) since this portion of the vagina, together with its attachments to the lumbar spine, acts against gravity without much help from the skeletal muscles of the pelvic floor. Skeletal muscles in the rats primarily serve to control the motion of the tails and do offer support to the viscera as in humans.

CONCLUSIONS

This study presents the first *in situ* quantification of smooth muscle orientation in the rat vagina while offering a qualitative description of the associated network of nerves. By using advanced tissue clearing techniques with immunohistochemistry staining, the three-dimensional architecture of the smooth muscle and nerves within the vagina was visualized, without sectioning and disrupting the morphology of the organ. The orientation distribution of VaSM was found to be bimodal, with VaSM primarily oriented along the LD and CD. The proximal vagina contained large regions of dense smooth muscle, and significantly more smooth muscle aligned along the LD than the CD. The mid vagina contained a scarce amount of smooth muscle while in the distal vagina the amount of VaSM along the LD and CD was comparable. These new data on the architecture of VaSM and nerves could have implications in diagnosis and treatment of female sexual dysfunction and pelvic floor disorders.

ACKNOWLEDGMENTS

Funding was provided by NSF Grant No. 1929731.

CONFLICT OF INTEREST

The authors declare that they have no conflict of interest.

REFERENCES

[1]Agostinelli, C. and U. Lund. R package circular: Circular statistics (version 0.4-93). CA: Department of Environmental Sciences, Informatics and Statistics, Ca' Foscari University, Venice, Italy. UL: Department of Statistics, California Polytechnic State University, San Luis Obispo, California, USA, 2017.

[2]Akintunde, A. R., K. M. Robison, D. J. Capone, L. Desrosiers, L. R. Knoepp, and K. S. Miller. Effects of elastase digestion on the murine vaginal wall biaxial mechanical response. *J. Biomech. Eng*. 141(2):0210111, 2019.

[3]Basha, M., S. Chang, E. M. Smolock, R. S. Moreland, A. J. Wein, and S. Chacko. Regional differences in myosin heavy chain isoform expression and maximal shortening velocity of the rat vaginal wall smooth muscle. *Am. J. Physiol. Regul. Integr. Comp. Physiol.* 291(4):R1076–R1084, 2006.

[4]Boreham, M. K., C. Y. Wai, R. T. Miller, J. I. Schaffer, and R. A. Word. Morphometric analysis of smooth muscle in the anterior vaginal wall of women with pelvic organ prolapse. *Am. J. Obstet. Gynecol.* 187(1):56–63, 2002.

[5]Boreham, M. K., C. Y. Wai, R. T. Miller, J. I. Schaffer, and R. A. Word. Morphometric properties of the posterior vaginal wall in women with pelvic organ prolapse. *Am. J. Obstet. Gynecol.* 187(6):1501–1509, 2002.

[6]Bredfeldt, J. S., Y. Liu, M. W. Conklin, P. J. Keely, T. R. Mackie, and K. W. Eliceiri. Automated quantification of aligned collagen for human breast carcinoma prognosis. *J. Pathol. Inform.* 5:28, 2014.

[7]Bredfeldt, J. S., Y. Liu, C. A. Pehlke, M. W. Conklin, J. M. Szulczewski, D. R. Inman, P. J. Keely, R. D. Nowak, T. R.

Mackie, and K. W. Eliceiri. Computational segmentation of collagen fibers from second-harmonic generation images of breast cancer. *J. Biomed. Opt.* 19(1):016007, 2014.
[8]Bø, K., and H. B. Finckenhagen. Is there any difference in measurement of pelvic floor muscle strength in supine and standing position? *Acta Obstet. Gynecol. Scand.* 82(12):1120–1124, 2003.
[9]Candes, E., L. Demanet, D. Donoho, and L. Ying. Fast discrete curvelet transforms. *Multiscale Model. Simul.* 5(3):861–899, 2006.
[10]Chanda, A., and V. Unnikrishnan. Effect of bladder and rectal loads on the vaginal canal and levator ani in varying pelvic oor conditions. *Mech. Adv. Mater. Struct.* 25(14):1214–1223, 2018.
[11]Clark, G. L., A. P. Pokutta-Paskaleva, D. J. Lawrence, S. H. Lindsey, L. Desrosiers, L. R. Knoepp, C. L. Bayer, R. L. Gleason Jr., and K. S. Miller. Smooth muscle regional contribution to vaginal wall function. *Interface Focus.* 9(4):20190025, 2019.
[12]Da Sacco, S., L. Perin, and R. E. De Filippo. Tissue Engineering of the Reproductive System, 2nd ed. San Diego: Academic Press, 2011.
[13]Daucher, J. A., K. A. Clark, D. B. Stolz, L. A. Meyn, and P. A. Moalli. Adaptations of the rat vagina in pregnancy to accommodate delivery. *Obstet. Gynecol.* 109(1):128–135, 2007.
[14]Faix, A., J. Lapray, O. Callede, A. Maubon, and K. Lanfrey. Magnetic resonance imaging (MRI) of sexual intercourse: Second experience in missionary position and initial experience in posterior position. *J. Sex Marital Ther.* 28(sup1):63–76, 2002.
[15]Feola, A., S. Abramowitch, Z. Jallah, S. Stein, W. Barone, S. Palcsey, and P. Moalli. Deterioration in biomechanical properties of the vagina following implantation of a high-stiffness prolapse mesh. *Int. J. Obstet. Gy.* 120(2):224–232, 2013.
[16]Feola, A., M. Endo, I. Urbankova, J. Vlacil, T. Deprest, S. Bettin, B. Klosterhalfen, and J. Deprest. Host reaction to vaginally inserted collagen containing polypropylene implants in sheep. *Am. J. Obstet. Gynecol.* 212(4):474, 2015.
[17]Giraldi, A., P. Alm, V. Werkström, L. Myllymäki, G. Wagner, and K.-E. Andersson. Morphological and functional characterization of a rat vaginal smooth muscle sphincter. *Int. J. Impot. Res.* 14(4):271, 2002.
[18]Giraldi, A., K. Persson, V. Werkström, P. Alm, G. Wagner, and K. Andersson. Effects of diabetes on neurotransmission in rat vaginal smooth muscle. *Int. J. Impot. Res.* 13(2):58, 2001.
[19]Goldstein, I. Female sexual arousal disorder: new insights. *Int. J. Impot. Res.* 12(4):S152–S157, 2000.
[20]Grozdanovic, Z., B. Mayer, H. G. Baumgarten, and G. Brüning. Nitric oxide synthase-containing nerve fibers and neurons in the genital tract of the female mouse. *Cell Tissue Res.* 275(2):355–360, 1994.
[21]Gruber, D. D., W. B. Warner, E. D. Lombardini, C. M. Zahn, and J. L. Buller. Anatomical and histological examination of the porcine vagina and supportive structures: In search of an ideal model for pelvic floor disorder evaluation and management. *Female Pelvic Med. Reconstr. Surg.* 17(3):110–114, 2011.
[22]Hilliges, M., C. Falconer, G. Ekman-Ordeberg, and O. Johansson. Innervation of the human vaginal mucosa as revealed by PGP 95 immunohistochemistry. *Cells Tissues Organs.* 153(2):119–126, 1995.
[23]Hoyle, C., R. Stones, T. Robson, K. Whitley, and G. Burnstock. Innervation of vasculature and microvasculature of the human vagina by nos and neuropeptide-containing nerves. *J. Anat.* 188(Pt 3):633, 1996.
[24]Huntington, A., S. D. Abramowitch, P. A. Moalli, and R. De Vita. Strains induced in the vagina by smooth muscle contractions. *Acta Biomater.* 129:178–187, 2021.
[25]Huntington, A., K. Donaldson, and R. De Vita. Contractile properties of vaginal tissue. *J. Biomech. Eng.* 2020. https://doi.org/10.1115/1.4046712.
[26]Huntington, A., E. Rizzuto, S. Abramowitch, Z. Del Prete, and R. De Vita. Anisotropy of the passive and active rat vagina under biaxial loading. *Ann. Biomed. Eng.* 47(1):272–281, 2019.
[27]Inal, H. A., P. B. Kaplan, U. Usta, E. Taştekin, A. Aybatlı, and B. Tokuc. Neuromuscular morphometry of the vaginal wall in women with anterior vaginal wall prolapse. *Neurourol. Urodyn.* 29(3):458–463, 2010.
[28]Jallah, Z., R. Liang, A. Feola, W. Barone, S. Palcsey, S. Abramowitch, N. Yoshimura, and P. Moalli. The impact of prolapse mesh on vaginal smooth muscle structure and function. *Int. J. Obstet. Gy.* 123(7):1076–1085, 2016.
[29]Kaplan, P. B., U. Usta, H. A. Inal, T. Tastekin, and B. Tokuc. Neuromuscular morphometry of the uterine ligaments and vaginal wall in women with pelvic organ prolapse. *Neurourol. Urodyn.* 30(1):126–132, 2011.
[30]Knight, K. M., A. M. Artsen, M. R. Routzong, G. E. King, S. D. Abramowitch, and P. A. Moalli. New Zealand white rabbit: a novel model for prolapse mesh implantation via a lumbar colpopexy. *Int. Urogynecol. J.* 31:91–99, 2020.
[31]Krantz, K. E. Innervation of the human vulva and vagina: a microscopic study. *Obstet. Gynecol.* 12(4):382–396, 1958.
[32]Mardia, K. V., and P. E. Jupp. Directional Statistics, Vol. 494, New York: Wiley, 2009.
[33]Martins, P., E. Peña, B. Calvo, M. Doblaré, T. Mascarenhas, R. Natal Jorge, and A. Ferreira. Prediction of nonlinear elastic behaviour of vaginal tissue: experimental results and model formulation. *Comput. Methods Biomech. Biomed. Eng.* 13(3):327–337, 2010.
[34]Mazloomdoost, D., L. B. Westermann, G. Mutema, C. C. Crisp, S. D. Kleeman, and R. N. Pauls. Histologic anatomy of the anterior vagina and urethra. *Female Pelvic Med. Reconstr. Surg.* 23(5):329–335, 2017.
[35]McGuire, J. A., S. D. Abramowitch, S. Maiti, and R. De Vita. Swine vagina under planar biaxial loads: an investigation of large deformations and tears. *J. Biomech. Eng.* 2019. https://doi.org/10.1115/1.4042437.
[36]McGuire, J. A., C. L. Crandall, S. D. Abramowitch, and R. De Vita. Inflation and rupture of vaginal tissue. *Interface Focus.* 9(4):20190029, 2019.
[37]Nagatomi, J., K. K. Toosi, J. S. Grashow, M. B. Chancellor, and M. S. Sacks. Quantification of bladder smooth muscle orientation in normal and spinal cord injured rats. *Ann. Biomed. Eng.* 33(8):1078–1089, 2005.
[38]Oh, S.-J., S. K. Hong, S. Kim, and J. Paick. Histological and functional aspects of different regions of the rabbit vagina. *Int. J. Impot. Res.* 15(2):142, 2003.
[39]Önol, F. F., F. Ercan, and T. Tarcan. The effect of ovariectomy on rat vaginal tissue contractility and histomorphology. *J. Sex. Med.* 3(2):233–241, 2006.
[40]Papka, R., J. Cotton, and H. Traurig. Comparative distribution of neuropeptide tyrosine-, vasoactive intestinal polypeptide-, substance p-immunoreactive, acetylcholinesterase-positive and noradrenergic nerves in the

reproductive tract of the female rat. *Cell Tissue Res.* 242(3):475–490, 1985.
[41]R Core Team. R: A Language and Environment for Statistical Computing. Vienna, Austria: R Foundation for Statistical Computing, 2021.
[42]Semmelink, H., P. de Wilde, J. van Houwelingen, and G. Vooijs. Histomorphometric study of the lower urogenital tract in pre-and post-menopausal women. *Cytometry A.* 11(6):700–707, 1990.
[43]Shabsigh, A., R. Buttyan, T. Burchardt, M. Buchardt, O. R. Hayek, V. D'Agati, C. Olsson, and R. Shabsigh. The microvascular architecture of the rat vagina revealed by image analysis of vascular corrosion casts. *Int. J. Impot Res.* 11(Suppl 1):S23–S30, 1999.
[44]Shaffer, R. M., R. Liang, K. Knight, C. M. Carter-Brooks, S. Abramowitch, and P. A. Moalli. Impact of polypropylene prolapse mesh on vaginal smooth muscle in rhesus macaque. *Am. J. Obstet. Gynecol.* 221:3301, 2019.
[45]Skoczylas, L. C., Z. Jallah, Y. Sugino, S. E. Stein, A. Feola, N. Yoshimura, and P. Moalli. Regional differences in rat vaginal smooth muscle contractility and morphology. *Reprod. Sci.* 20(4):382–390, 2013.
[46]Song, Y. B., K. Hwang, D. J. Kim, and S. H. Han. Innervation of vagina: microdissection and immunohistochemical study. *J. Sex Marital Ther.* 35(2):144–153, 2009.
[47]Spronck, B., R. T. Megens, K. D. Reesink, and T. Delhaas. A method for three-dimensional quantification of vascular smooth muscle orientation: Application in viable murine carotid arteries. *Biomech. Model. Mechanobiol.* 15(2):419–432, 2016.
[48]Stein, A. M., D. A. Vader, L. M. Jawerth, D. A. Weitz, and L. M. Sander. An algorithm for extracting the network geometry of threedimensional collagen gels. *J. Microsc.* 232(3):463–475, 2008.
[49]Takacs, P., M. Gualtieri, M. Nassiri, K. Candiotti, A. Fornoni, and C. A. Medina. Caldesmon expression is decreased in women with anterior vaginal wall prolapse: a pilot study. *Int. Urogynecol. J.* 20(8):985–990, 2009.
[50]Takacs, P., M. Gualtieri, M. Nassiri, K. Candiotti, and C. A. Medina. Vaginal smooth muscle cell apoptosis is increased in women with pelvic organ prolapse. *Int. Urogynecol. J.* 19(11):1559, 2008.
[51]Tan, T., and R. De Vita. A structural constitutive model for smooth muscle contraction in biological tissues. *Int. J. Non Linear Mech.* 75:46–53, 2015.
[52]Ting, A. Y., A. D. Blacklock, and P. G. Smith. Estrogen regulates vaginal sensory and autonomic nerve density in the rat. *Biol. Reprod.* 71(4):1397–1404, 2004.
[53]Vetuschi, A., A. D'Alfonso, R. Sferra, D. Zanelli, S. Pompili, F. Patacchiola, E. Gaudio, and G. Carta. Changes in muscularis propria of anterior vaginal wall in women with pelvic organ prolapse. *Eur. J. Histochem.* 60(1):2604, 2016.
[54]Watson, G. S. Goodness-of-fit tests on a circle. *Biometrika.* 48(1/2):109–114, 1961.
[55]Zhu, L., J. Lang, J. Chen, and J. Chen. Study on nerve fiber density in anterior vaginal epithelium for stress urinary incontinence. *Int. Urogynecol. J.* 15(4):272–275, 2004.